Optical Materials 31 (2008) 268–275

Contents lists available at ScienceDirect

Optical Materials

journal homepage: www.elsevier.com/locate/optmat

Efficient green luminescence in Tb^{3+}-activated borates, $A_6MM'(BO_3)_6$

R. Sankar *

Phosphor Laboratory, Materials Science Division, Central Electrochemical Research Institute, Karaikudi 630 006, Tamilnadu, India

ARTICLE INFO

Article history:
Received 6 November 2007
Received in revised form 12 January 2008
Accepted 7 April 2008
Available online 29 May 2008

ABSTRACT

Photoluminescence of several new green-emitting Tb^{3+}-activated borates of the type $Sr_6MM'(BO_3)_6$ [A = Sr; M = Gd, Y; M′ = Al, Ga, In, Sc, Y] and $LaSr_5MM'(BO_3)_6$ [A = Sr, La; M = Y; M′ = Mg] with Tb^{3+} at the M or M′ site has been studied and the results are presented here. All these borates are synthesized by the solid state reactions under reducing atmospheres and are characterized by powder XRD, density, TG/DT, particle size analysis and photoluminescence techniques. These borates are synthesizable at temperatures below 1000 °C as evidenced by thermal studies and are found to have narrow range of particle sizes (5–15 μm). The photoluminescence excitation spectra of these borates show a broad band at ~257 nm due to 4f–5d transition of Tb^{3+} ion, which also depends on Tb^{3+} concentration. Under excitation with 254 nm, all these borates display high intense green emission at 542 nm due to $^5D_4$–$^7F_5$ transition of Tb^{3+} ion. The influence of ions doped at the M′-site on the luminescence of Tb^{3+} is also studied. The luminescence properties of all these borates have been compared with each other and with the standard phosphor, $LaCePO_4$:Tb^{3+}. The results show that these borate phosphors have several advantages over the standard green phosphors. Thus, the group of Tb^{3+}-activated hexaborate phosphors is an efficient alternative to the existing commercial green phosphors for use in tri-color low pressure mercury vapor lamps.

1. Introduction

Several new green phosphors for use in tri-color low pressure mercury vapor lamps have been reported in the past decades and some of them are commercialized [1–3]. The pre-requisites of commercial phosphors are mainly low cost and efficient performance during lamp applications. The cost-reduction can be achieved by the choice of host lattices. That is, by choosing host lattices which can be synthesized at lower temperatures and which do not require expensive raw materials for their syntheses. The performance and efficiency of phosphors during lamp application depend on many factors [3]. In the lab scale, it is necessary to investigate the performance of new phosphors by comparing their luminescence properties with the standard phosphors. The known commercial standards are the green-emitting $CeMgAl_{11}O_{19}$:Tb^{3+}, $GdCeMgB_5O_{10}$:Tb^{3+} and $LaCePO_4$:Tb^{3+} [2]. The phosphors $CeMgAl_{11}O_{19}$:Tb^{3+} and $LaCePO_4$:Tb^{3+} require high processing temperatures, high reducing atmospheres and high Tb^{3+} concentrations, for efficient performance. The aluminate and phosphate phosphors require high reducing atmospheres when compared to the present borates to reduce Tb^{4+} to Tb^{3+} because of differences in their crystal structure and the ionic environment. In practice it is understood that the reduction is enhanced in borate anionic networks under mild-reducing atmospheres when compared to phosphate or aluminate networks. The borate phosphor $GdMgB_5O_{10}$:Tb^{3+} does not require very high temperatures like the aluminate or the phosphate phosphors, but, to reduce Tb^{3+} concentration the borate requires the ion Ce^{3+} as sensitizer. The presence of the ion Ce^{3+} in all these phosphors causes instability if heated in air at room and at high temperatures, and hence causes problem during the baking process of lamp fabrication. To overcome these difficulties, a phosphor with a stable Tb^{3+} state which is capable of undergoing excitation with radiation of wavelength 254 nm (so as to avoid sensitizers like Ce^{3+} ion) and which can be synthesized at lower temperatures in air/mild-reducing atmospheres is needed. Our attempts on different host lattices led to the invention of the new Tb^{3+}-activated (at the M or M′-sites) borates of the type $A_6MM'(BO_3)_6$ [A = Sr; M = Gd, Y; M′ = Al, Ga, In, Sc and Y] and $LaSr_5MM'(BO_3)_6$ [A = Sr, La; M = Y; M′ = Mg] [4–7] which can be used as alternatives to the above commercial green phosphors after suitable modifications.

Our early studies on the luminescence properties of Tb^{3+} doped hexaborates of the type $A_6MM'(BO_3)_6$ have shown very promising results and were published elsewhere [8]. In this paper we report the synthesis, characterization and the luminescence properties of the new Tb^{3+}-activated hexaborates in detail owing to their potential for application. The suitability of these phosphors for application in low pressure mercury vapor (lpmv) lamps has also been discussed.

* Present address: PDP Division, SAMTEL COLOR Limited, Village Chhapraula, Bulandshahar Road, Ghaziabad 201 009, UP, India. Tel.: +91 9818641828.
E-mail address: ram.sankar@rediffmail.com

0925-3467/$ - see front matter © 2008 Elsevier B.V. All rights reserved.
doi:10.1016/j.optmat.2008.04.003

2. Experimental

The samples in polycrystalline form (up to a bulk of 30 g) were synthesized by the conventional high temperature solid state reactions. The starting materials were: RE_2O_3 (RE = Y, La, Gd), Tb_4O_7 all of 99.99% purity (Indian Rare Earths Ltd), Sc_2O_3, Ga_2O_3, In_2O_3 (99.99% all cerac), $SrCO_3$ (99.5% Lumichem Ltd.) H_3BO_3 (99.5%, Glaxo (India) Ltd), MgO (>98%, BDH, England) and $Al(NO_3)_3 \cdot 9H_2O$ (>98.5%, Thomas Baker Ltd). La_2O_3 was heated in air at 1000 °C for 24 h to remove the moisture and CO_2 present in it and kept in a desiccator. The starting materials were thoroughly homogenized in an agate mortar and then transferred into alumina crucibles for heat treatment in a muffle furnace. An excess of 3–5 mol% H_3BO_3 was added to compensate for any loss due to vaporization. An excess of 1 mol% $Al(NO_3)_3 \cdot 9H_2O$ was added to compensate for any weight loss. The heat treatment was carried out under reducing atmosphere created by NH_3 decomposition (N_2:$3H_2$) for about 10–30 h at temperatures ranging from 900 to 1150 °C. In addition the pressure of this forming gas was maintained constant throughout the reaction. All the compounds were cooled inside the furnace to room temperature by furnace shut-off, before being taken out.

Powder X-ray diffractograms (XRD) of the compounds were obtained using a JEOL JDX 8030 powder X-ray diffractometer employing Cu K_α-radiation with Ni filter (scan speed 0.1 deg s^{-1}). The observed (*hkl*) reflections were compared with the calculated ones generated using the computer program LAZY PULVERIX for the different compositions. The crystal data and atom positions were taken from Ref. [5]. The lattice parameters were calculated from the indexed XRD patterns using least-squares refinement. Powder density measurements were calculated using pycnometric technique with xylene as the medium. A 10 ml specific gravity bottle and about 1 g of sample were used for measurement. The thermal analysis measurements (TG/DTA) were carried out in N_2 atmosphere (in the range 25–1000 °C, 10 °C/min) using a simultaneous thermal analysis system (STA 1500; PL Thermal Sci. Ltd., UK). Particle size analysis was carried out using a MALVERN particle sizer 3600E type (Malvern Instruments; England). The photoluminescence excitation and emission spectra were recorded at room temperature using a Hitachi 650-10S fluorescence spectrophotometer equipped with a 150 W Xenon lamp and a Hamamatsu R928F photomultiplier detector. The instrument has been calibrated externally using standard phosphors. The spectra recorded after calibration of the instrument were presented in the paper. The spectral sensitivity of the instrument is high in the visible region especially in the green region. The integrated emission intensity measurements were carried out for samples taken in equal amounts and prepared under identical conditions. For comparison purposes, the commercial sample of the green phosphor LaCe-PO_4:Tb^{3+} was used (NICHIA Co., Japan).

3. Results and discussion

The compounds are crystalline solids, white in color, stable in air and are insoluble in water. The XRD patterns establish the single phase nature of the synthesized compounds and no second phase was noted. The powder XRD pattern for the compound $Sr_6YTb(BO_3)_6$ is shown in Fig. 1 and the powder XRD data in Table 1. The least-squares fit hexagonal lattice parameters of the above compound are $a = 12.51$ Å and $c = 9.26$ Å against the values $a = 12.503$ Å and $c = 9.248$ Å for the compound $Sr_6YY(BO_3)_6$ reported in Ref. [5]. The powder density of the compound $Sr_6Y_{1.9}Tb_{0.1}(BO_3)_6$ (meas. = 4.08 g ml^{-1}, theor. = 4.20 g ml^{-1}) obtained by the pycnometric technique is found to be >97% of the theoretical density. The thermal studies (TG/DT) carried out on the starting materials of the compound $Sr_6YTb(BO_3)_6$ in N_2 atmosphere show a sharp endotherm (DTA) at 690 °C (±10 °C) supported by a weight loss (TG) at that temperature confirming the formation of the compound at 690 °C (±10 °C) (Fig. 2). In addition, the thermal studies on the already formed $Sr_6YTb(BO_3)_6$ in N_2 atmosphere indicate no phase transition or weight loss in the range 25–1000 °C. The particle size analysis of the compound $Sr_6YTb(BO_3)_6$ shows that the sizes of the particles are in the range 5–15 μm.

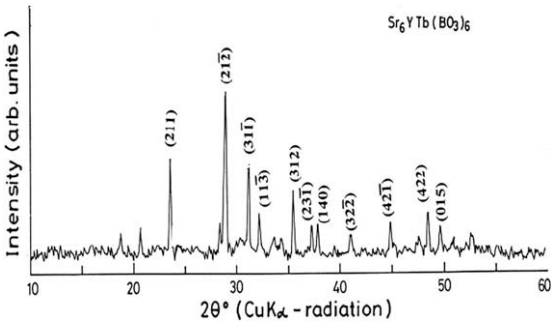

Fig. 1. Powder X-ray diffraction pattern of the compound $Sr_6YTb(BO_3)_6$ (Cu K_α-radiation).

Table 1
Powder XRD data of $Sr_6YTb(BO_3)_6$ compound (Cu K_α radiation)

d_{exptl}	d_{std}[a]	$I/I_{0\ exptl.}$	$I/I_{0\ std.\ std.}$[a]	(*hkl*) [a]
3.751	3.745	50	65	211
3.066	3.067	100	100	21-2
2.855	2.858	67	50	31-1
2.753	2.768	25	10	11-3
2.513	2.520	36	32	312
2.396	2.400	15	17	23-1
2.360	2.364	25	20	140
2.189	2.189	15	5	32-2
2.004	2.015	25	7	42-1
1.868	1.872	23	7	422
1.826	1.825	12	6	015

Rhombohedral-hexagonal system; Hexagonal space-group: $R\bar{3}$; Least-squares fit lattice parameters: $a = 12.51$ Å and $c = 9.26$ Å against the values $a = 12.503$ Å and $c = 9.248$ Å for the compound $Sr_6YY(BO_3)_6$ reported in Ref. [5]. It is to be noted that (*hkl*) are the Miller indices, *I* is the intensity in arbitrary unit and *d* is the interplanar spacing in Å.

[a] Obtained by alternating between the software programs LAZY PULVERIX (A program to generate powder XRD data from single crystal data) and HOCT (A program to calculate the values of lattice parameters from the experimental powder XRD data, by applying the method of least squares).

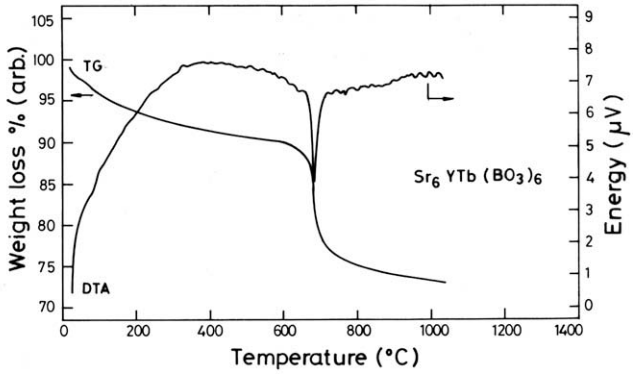

Fig. 2. Thermal analysis (TG/DT) curves of the starting materials for the formation of the compound $Sr_6YTb(BO_3)_6$ recorded in N_2 atmosphere in the temperature range 25–1000 °C (Starting materials: $SrCO_3$, Y_2O_3, Tb_4O_7 and H_3BO_3 → $Sr_6YTb(BO_3)_6$ + H_2O + gases).

3.1. Tb^{3+} luminescence – general

The efficient green luminescence of Tb^{3+} in many compounds is well-known and extensively studied [9–16]. It is also known that the ion Tb^{3+} has relatively simple 4f-configurational energy levels with ^7F_J ($J = 6, \ldots, 0$) ground states and ^5D_J ($J = 4, 3$) excited states and are responsible for efficient luminescence in many host lattices. Normally, the absorption/excitation spectrum of Tb^{3+} ion consists of two broad bands, one towards higher energy side (spin-allowed 4f–5d transition to the ^7D level of Tb^{3+} ion), the other at lower energy side (spin-forbidden 4f–5d transition to ^9D level) and the $4f^8$ (f–f) excitation lines [9,16]. The energy difference between the spin-allowed and spin-forbidden transitions is around 4700 cm^{-1}, and the ratio of their intensities is around 50 [17]. Of all the excitation bands of Tb^{3+}, the band due to spin-allowed transition will be of high intensity.

The emission spectrum of Tb^{3+} ions in crystals shows sharp lines due to transitions between $^5D_{J=3,4}$ and $^7F_J = 0, 1, \ldots, 6$ states. At low Tb^{3+} concentrations (<5 mol% normally), only emissions due to $^5D_3$–^7F_J transition are present when excited with energies corresponding to the $4f^8$ excitation levels (direct excitation of $4f^8$ levels). This is usually due to the large energy gap between $^5D_3$ and $^5D_4$ levels of Tb^{3+} which amounts to about 5500 cm^{-1}. At higher Tb^{3+} concentrations ($\geqslant$5 mol%), the mean Tb^{3+}–Tb^{3+} distance will decrease and hence there will be energy transfer *via* cross-relaxation between $^5D_3$ and $^5D_4$ levels ($^5D_3 \rightarrow {}^5D_4$ and $^7F_6 \rightarrow {}^7F_0$, $^5D_3 \rightarrow {}^7F_0$ and $^7F_6 \rightarrow {}^5D_4$) [18]. Hence, if the Tb^{3+} concentration is increased gradually from low to high, $^5D_3$ emission will be quenched and the emission from $^5D_4$ level will increase gradually in intensity. Thus, at higher Tb^{3+} concentrations, the $^5D_4$–^7F_J (green) emissions are dominant and $^5D_3$–^7F_J (blue) emissions are quenched. The excitation energies corresponding to the $4f^7$-5d transition bands (direct excitation of $4f^7$–5d) results in $^5D_4$–^7F_J (green) emissions because the excited electron relaxes directly from the $4f^7$5d state to the $^5D_4$ level feeding it directly [18,19]. The process of cross-relaxation mainly depends on the energy of the available phonons, crystal field and index of refraction [9]. The transition $^5D_4$–$^7F_6$ is hypersensitive to the surroundings. But when compared to Eu^{3+} ion, Tb^{3+} ion is less sensitive. The maximum quantum efficiency of a Tb^{3+}-doped phosphor is determined by the deviation from inversion symmetry of the Tb^{3+}-ion-site and the energy position of the $4f^7$–5d excitation band of Tb^{3+} ion [10]. The larger is the deviation from inversion symmetry and the longer is the wavelength position of the 4f–5d band, the lower is the quantum efficiency.

3.2. $Sr_6YY(BO_3)_6$:Tb^{3+} (at the Y-site)

Compounds of the form $Sr_6Y_{1-x}Tb_xY(BO_3)_6$ (hereafter referred to as D) with M = M′ = Y and $x = 0.05$–1.0 were synthesized and photoluminescence measurements were carried out for all compositions. However, only the low (0.05) and high (0.25) concentrations were considered to facilitate a comparison of the spectra. In the compound $Sr_6Y_{1-x}Tb_xY(BO_3)_6$, it is possible for the Tb^{3+} ion to occupy both the M and M′-sites due to the flexibility of the ionic sites in the crystal lattice [5]. The crystal structure of the presently studied borates is such that the ionic sites are capable of accommodating variety of ions of different ionic radii, both larger and smaller. Hence this shows the flexibility of ionic sites, especially those of M and M′ sites in the crystal borate. The excitation spectrum recorded at $T = 300$ K for the compound D with $x = 0.05$ (Fig. 3a) shows a broad band peaking at 240–245 nm and is due to $4f^7$–5d transition of Tb^{3+} ion. This transition can be assigned to the spin-forbidden transition owing to its lower energy position when compared to the spin-allowed transition which normally will appear around 200–220 nm [9,16]. There is a shoulder at 280–285 nm on this band with very low intensity, which may be due to crystal field.

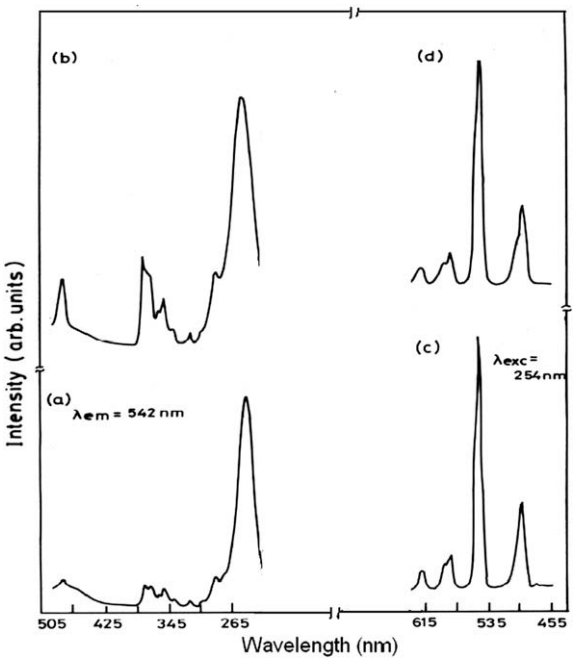

Fig. 3. Room temperature excitation (a, b) and emission (c, d) spectra of $Sr_6Y_{1-x}Tb_x(BO_3)_6$ recorded for two different values of x [$x = 0.05$ (a, c) and $x = 0.25$ (b, d)]. The excitation and emission wavelengths are shown.

The $4f^8$-excitation lines are present in the range 325–505 nm with very weak intensity when compared to the spin-forbidden excitation band. The excitation line at 385 nm is due to the $^7F_6$–$^5L_{10}$ transition and the line at 350 nm is due to $^7F_6$–$^5D_2$ transition of Tb^{3+} ion.

When the Tb^{3+} concentration is increased to 0.25 and above, *i.e.*, for $x = 0.25$–1.0, the peak of the excitation band shifts towards 255–260 nm (Fig. 3b). All the other excitation lines observed are present at the respective positions similar to the case encountered for D with $x = 0.05$. The position of the excitation band is indicative of many possible features. First of all, the host lattice doped with Tb^{3+} ion can be efficiently excited with radiation of wavelength 254 nm, the required excitation wavelength for application in low pressure mercury vapor lamps. The energy position of $4f^7$–5d band also indicates that the Tb^{3+} ion-site (M or M′-site here) is of high symmetry. It also indicates the electro negativity of the hexaborate lattice [9].

The emission spectrum recorded for D with $x = 0.05$ under 254 nm excitation gives only the lines corresponding to transitions from the $^5D_4$ level (Fig. 3c). The emission lines seen in the spectrum are the $^5D_4$–$^7F_3$ transition at 620 nm, the $^5D_4$–$^7F_4$ transition at

Table 2
Comparison of the integrated emission intensities of the presently synthesized hexaborate green phosphors ($\lambda_{exc} = 254$ nm)

Composition	Excitation peak (nm)	Emission peak (nm)	Integrated intensity[a] (%)
$Sr_6YTb(BO_3)_6$	257	542	78
$Sr_6Gd_{1.5}Tb_{0.5}(BO_3)_6$	257	542	80
$Sr_6TbTb(BO_3)_6$	257	542	70
$Sr_6TbAl(BO_3)_6$	238, 268[b], 285	542[b], 545	66
$Sr_6TbGa(BO_3)_6$	238, 268[b], 285	542[b], 545	62
$Sr_6TbIn(BO_3)_6$	238, 268[b], 285	542[b], 545	55
$Sr_6TbSc(BO_3)_6$	257	542	70
$LaSr_5TbMg(BO_3)_6$	245, 265[b], 285	542[b], 545	62

[a] The value obtained for the standard green phosphor, $LaCePO_4$:Tb^{3+} under 254 nm excitation is taken as 100.
[b] High intense peak.

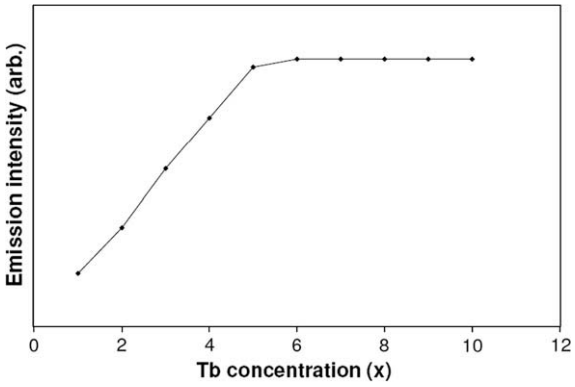

Fig. 4. Emission intensity *vs.* Tb concentration in $Sr_6Y_{1-x}Tb_x(BO_3)_6$ showing the saturation behavior (λ_{exc} = 254 nm).

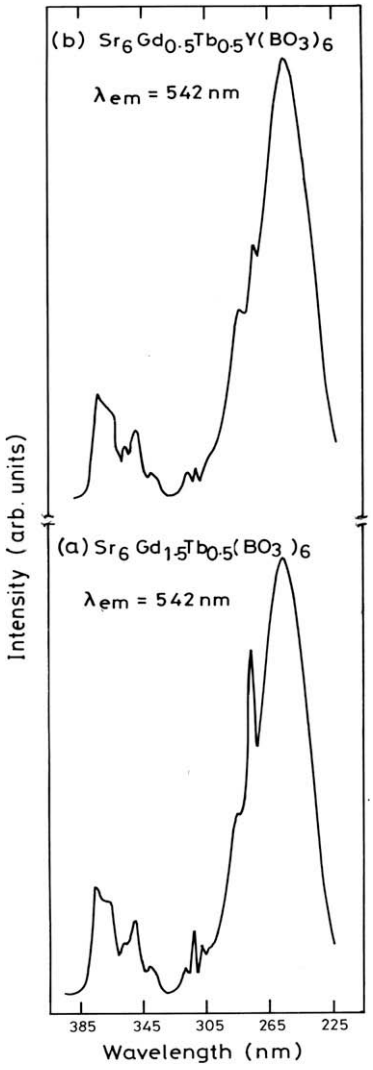

Fig. 5. Excitation spectra of (a) $Sr_6Gd_{1.5}Tb_{0.5}(BO_3)_6$ and (b) $Sr_6Gd_{0.5}Tb_{0.5}Y(BO_3)_6$. λ_{em} = 542 nm.

582 nm, the $^5D_4$–$^7F_5$ transition at 542 nm and the hyper-sensitive $^5D_4$–$^7F_6$ transition at 490 nm. Of all the emission lines, the line due to the $^5D_4$–$^7F_5$ transition at 542 nm is of highest intensity. Hence, the compound D gives green emission. No blue emission due to transition from $^5D_3$ level is observed. It is clear that the

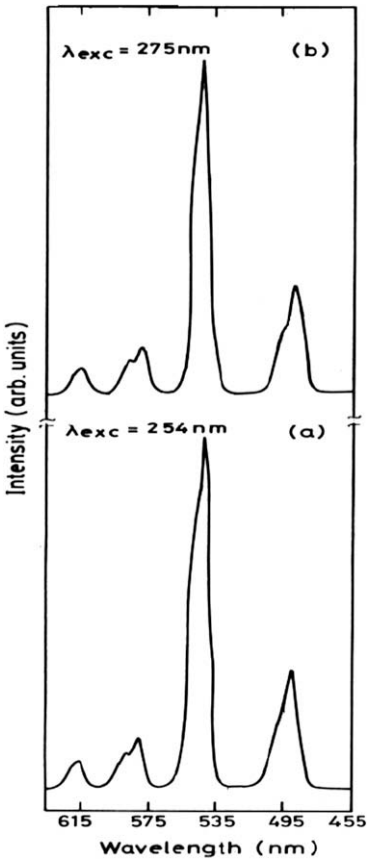

Fig. 6. Emission spectra of $Sr_6Gd_{1.5}Tb_{0.5}(BO_3)_6$ recorded for two different excitation wavelengths: (a) λ_{exc} = 254 nm (Tb^{3+} excitation) and (b) λ_{exc} = 275 nm (Gd^{3+} excitation).

$^5D_3$ emissions are quenched due to rapid multiphonon relaxation between $^5D_3$ and $^5D_4$ states owing to the high (phonon) vibrational frequency of the borate lattice.

The emission spectrum recorded for D with $x = 0.25$ under 254 nm excitation gives all the lines corresponding to the respective transitions $^5D_4$–^7F_J (J = 3–6) as observed for D with $x = 0.05$ (Fig. 3d). As the concentration of Tb^{3+} activated at the Y-site is increased, the emission intensity increases in D with x = 0.25–1.0, but the spectra looks similar to each other. Usually, the ratio of the emission intensities of $^5D_4$–^7F_J (J = 5, 4, 3) transitions will be 89:1:10 [9]. But in the compounds D with x = 0.05–1.0, the emission intensity due to transition $^5D_4$–$^7F_3$ is the lowest and the intensity due to transition $^5D_4$–$^7F_5$ is the highest. Thus, the contribution to the integrated emission intensity from transitions other than $^5D_4$–$^7F_5$ is much lower and only the green emission due to $^5D_4$–$^7F_5$ transition contributes to the total intensity. Since the compounds D with x = 0.05–1.0 have the $4f^7$–5d excitation band which peaks at ~257 nm, the compounds D do not require any sensitizer(s) like Ce^{3+} which is unstable when heated in air at high temperature. In addition, the compounds D with x = 0.05–1.0 give intense green emission under 254 nm excitation, similar to the $LaCePO_4$:Tb^{3+} green phosphor. The integrated emission intensity of D with x = 1.0 under 254 nm excitation is 78% of the intensity of the standard green phosphor $LaCePO_4$:Tb^{3+} under this excitation (Table 2). In addition, the variation in emission intensity with Tb concentration in D clearly shows saturation behavior with an optimum value for x at 0.5 (Fig. 4). Hence, the compound D has good potential for use in tri-color lpmv lamps as green component.

When the Tb^{3+} concentration (x) in D is increased to 2, *i.e.*, when x = 2, a compound of the type $Sr_6TbTb(BO_3)_6$ is formed. The excitation

and emission features of this compound are similar to those of D with $x = 0.25–1.0$ (not shown in Fig. 3). The integrated emission intensity of $Sr_6TbTb(BO_3)_6$ under 254 nm excitation is about 70% of the value obtained for the standard phosphor $LaCePO_4:Tb^{3+}$ (Table 2).

3.3. $Sr_6GdGd(BO_3)_6:Tb^{3+}$ (at the Gd-site)

Compounds of the form $Sr_6Gd_{1.5}Tb_{0.5}(BO_3)_6$ (hereafter referred to as E) have been prepared to study the possible energy transfer *via* Gd^{3+} ions. It is difficult to understand the repartition of the Gd and Y ions at the M and M′-sites, but can be concluded on the basis of the differences in their ionic sizes in these borates. This is because of the preferential occupation of M-site by ions of larger ionic radii and the M′-site by ions of smaller ionic radii as necessitated by the crystal structure of these hexaborates [5]. The excitation spectrum recorded for E gives the high intense broad band due to the $4f^7–5d$ transition which peaks at 255–260 nm (Fig. 5a). The Gd^{3+} excitation line due to the $^8S–^6I$ transition appears as a shoulder on the broad excitation band at 275 nm. In addition, one more shoulder appears at 285 nm on the broad excitation band which may be due to the crystal field. The shoulders are very low in intensity when compared to the excitation band. When the Gd^{3+} ion in B is diluted with yttrium (Y^{3+}) to form a compound of the form $Sr_6Gd_{0.5}Tb_{0.5}Y(BO_3)_6$ (hereafter referred to as F) and scanned for excitation, the excitation spectrum shows similar features to that of E, but the $^8S–^6I$ transition gives low intensity due to low Gd^{3+} concentration in F, when compared to E (Fig. 5b). The emission spectrum of $Sr_6Gd_{1.5}Tb_{0.5}(BO_3)_6$ shows the usual $^5D_4–^7F_J$ ($J = 3$, 4, 5, 6) transitions of Tb^{3+} at the respective positions previously observed for D, and the line due to $^5D_4–^7F_5$ transition is of high intensity (Fig. 6a). The emission spectrum of E has also been recorded for excitation with 275 nm (Gd^{3+} excitation) to check energy transfer between Gd and Tb ions. The spectra under excitation with 275 nm shows all the Tb^{3+} emission lines similar to E with

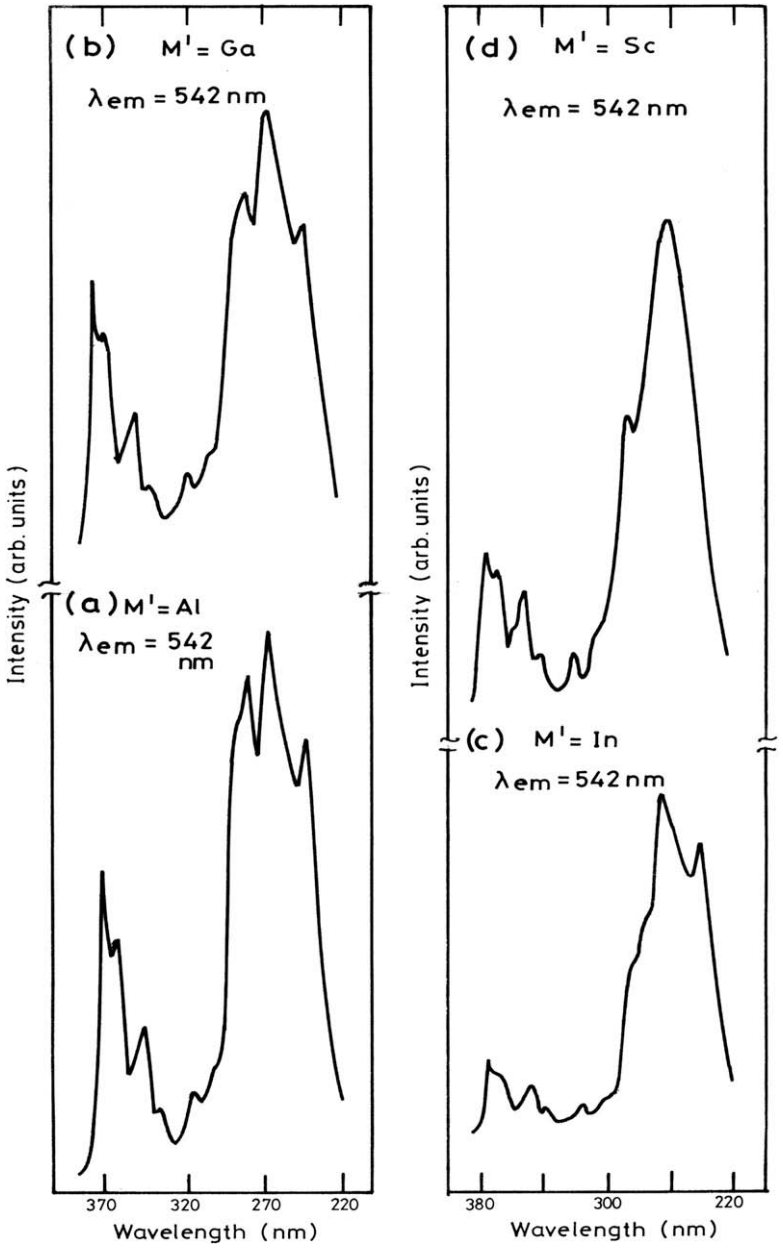

Fig. 7. Excitation spectra of (a) $Sr_6TbAl(BO_3)_6$, (b) $Sr_6TbGa(BO_3)_6$, (c) $Sr_6TbIn(BO_3)_6$ and (d) $Sr_6TbSc(BO_3)_6$. $\lambda_{em} = 542$ nm.

254 nm excitation (Fig. 6b). This clearly indicates the energy transfer from Gd^{3+} to Tb^{3+} *via* Gd^{3+} sub-lattice, in the compounds E and F [20]. As a result, the integrated emission intensity of E under 254 nm excitation is about 80% of the integrated emission intensity of $LaCePO_4$:Tb^{3+} (Table 2).

3.4. $Sr_6TbM'(BO_3)_6$ (M′ = Al, Ga, In, Sc)

Compounds of the form $Sr_6TbM'(BO_3)_6$ with M′ = Al, Ga, In, Sc were synthesized and their luminescence studied in order to check the influence of the ions present at the M′-site on the Tb^{3+} luminescence of these compounds. Unlike D and E, here Tb^{3+} prefers to occupy only the M-site (due to its larger ionic size when compared to the ionic sizes of Al, Ga, In and Sc) owing to the crystal structure of the hexaborate lattice [5]. The excitation spectrum recorded for $Sr_6TbAl(BO_3)_6$ (M′ = Al) gives the broad band due to which peaks at 268 nm and the other $4f^8$ excitation lines (Fig. 7a). Contrary to the bands observed in D and E, the excitation band of $Sr_6TbAl(BO_3)_6$ shows three splittings in its peak. Thus, the band appears to have three sharp peaks of which the peak at 268 nm is of high intensity (Fig. 7a and Table 2). One possible reason for these splittings is the crystal field of the lattice surrounding the ion. Another reason is the overlap of two or more excitation bands originating from the Tb^{3+}-ions occupying different unequivalent sites (M and M′). Similar is the case observed for $Sr_6TbGa(BO_3)_6$ (M′ = Ga) and $Sr_6TbIn(BO_3)_6$ (M′ = In) (Fig. 7b and c).

The excitation spectrum observed for the compound $Sr_6TbSc(BO_3)_6$ (M′ = Sc) gives the spin-forbidden transition at ~258 nm similar to the case encountered for the compounds A and B (Fig. 7d). No splittings are observable in the excitation band. The f–f excitation lines are present in the respective positions as shown in Fig. 7d.

Emission spectrum of $Sr_6TbAl(BO_3)_6$ recorded for excitation with 254 nm gives $^5D_4$–^7F_J (J = 3–6) transitions at the respective positions previously observed for D and E. The emission due to $^5D_4$–$^7F_5$ transition at 542 nm is of high intensity, and the others

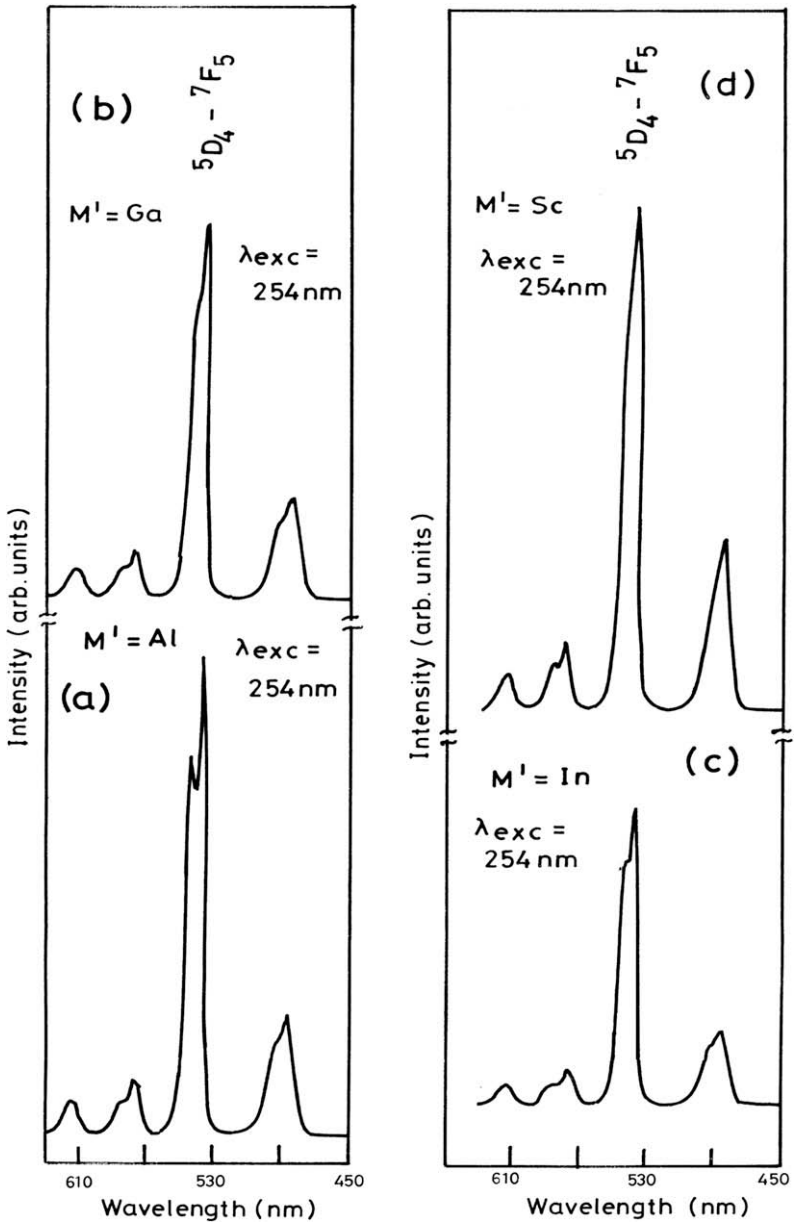

Fig. 8. Emission spectra of (a) $Sr_6TbAl(BO_3)_6$, (b) $Sr_6TbGa(BO_3)_6$, (c) $Sr_6TbIn(BO_3)_6$ and (d) $Sr_6TbSc(BO_3)_6$. λ_{exc} = 254 nm.

are weak in intensity (Fig. 8a). The peak of the $^5D_4$–$^7F_5$ transition shows two splitting (~3 nm difference). This splitting is not observed in the emission spectrum of the compounds D and E. The emission spectra of $Sr_6TbGa(BO_3)_6$ and $Sr_6TbIn(BO_3)_6$ look similar to that of $Sr_6TbAl(BO_3)_6$ (Fig. 8b and c). The emission spectrum recorded with 254 nm excitation for $Sr_6TbSc(BO_3)_6$ is similar to that of the compounds D and E, and does not show any splitting in the $^5D_4$–$^7F_5$ transition. The integrated emission intensities of $Sr_6TbM'(BO_3)_6$ with M′ = Al, Ga, In and Sc, under 254 nm excitation are given in Table 2. All these compounds give efficient green emission under 254 nm excitation and hence these borates are suitable candidates for use as efficient green components in tri-color lpmv lamps.

3.5. $LaSr_5YMg(BO_3)_6:Tb^{3+}$ (at the Y-site)

Compounds of the form $LaSr_5Y_{0.9}Tb_{0.1}Mg(BO_3)_6$ and $LaSr_5TbMg(BO_3)_6$ have been synthesized and their luminescence studied. The compound with (La, Sr) at the A-site is one of the derivatives of this system of borates. The investigation on this system is carried out to know whether the luminescence properties of terbium in this compound is influenced by the presence of larger La ion at the A-site and smaller Mg ion at M′-site. The excitation spectrum recorded for $LaSr_5Y_{0.9}Tb_{0.1}Mg(BO_3)_6$ gives the 4f–5d spin-forbidden transition which peaks at 238 nm, the shoulder at 285 nm and the $4f^8$ excitation lines up to 385 nm (Fig. 9a). When the concentration of Tb^{3+} is increased *i.e.*, for the compound $LaSr_5TbMg(BO_3)_6$, the peak of the excitation band shifts towards 245 nm (Fig. 9b). The band contains shoulders at 265 nm and 285 nm.

The emission spectrum recorded for $LaSr_5Y_{0.9}Tb_{0.1}Mg(BO_3)_6$ under 254 nm excitation gives lines corresponding to the $^5D_4$–^7F_J (J = 3–6) transitions (Fig. 10a). The $^5D_4$–$^7F_5$ transition is of high intensity and it does not show any splitting. When the excitation wavelength is changed to 238 nm, the emission spectrum obtained shows similar features to that obtained for excitation with 254 nm, but the $^5D_4$–$^7F_5$ transition shows sharp splitting (Fig. 10b). The emission spectrum of the compound $LaSr_5TbMg(BO_3)_6$ under 254 nm excitation looks similar to that obtained for $LaSr_5Y_{0.9}Tb_{0.1}Mg(BO_3)_6$ but the intensity of excitation and emission bands are high when compared to $LaSr_5Y_{0.9}Tb_{0.1}Mg(BO_3)_6$ (Table 2).

3.6. Advantages

It is clear from the Table 2 that the hexaborate phosphors have their emission intensities which is about 70–80% of the intensity of the standard $LaCePO_4:Tb^{3+}$ phosphor. Hence, these borate phosphors have excellent potential for application as green components in tri-color lpmv lamps, even though the intensity values are lower than those of $LaCePO_4:Tb^{3+}$. In addition to the high values of their integrated emission intensities, these borates have several other advantages, as detailed below.

(a) These hexaborates have the excitation band peaking at ~257 nm and is of very high intensity. Hence, these borates can be efficiently excited with light of wavelength 254 nm

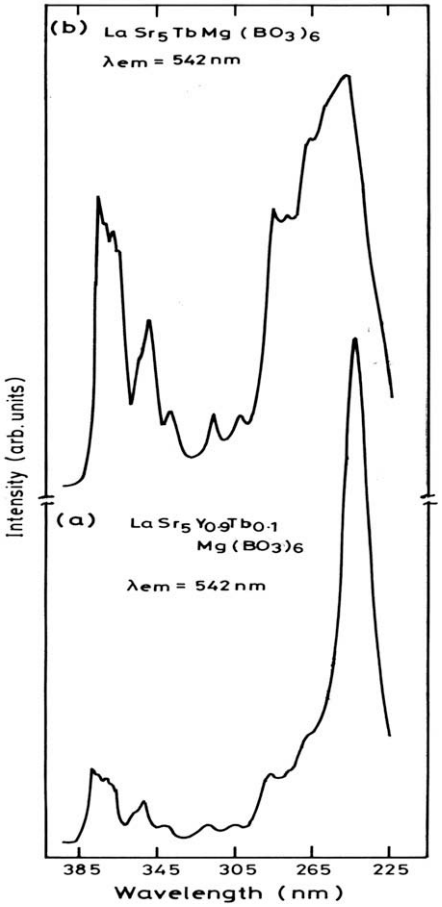

Fig. 9. (a) Excitation spectra of $LaSr_5Y_{0.9}Tb_{0.1}Mg(BO_3)_6$ and (b) $LaSr_5TbMg(BO_3)_6$. λ_{em} = 542 nm.

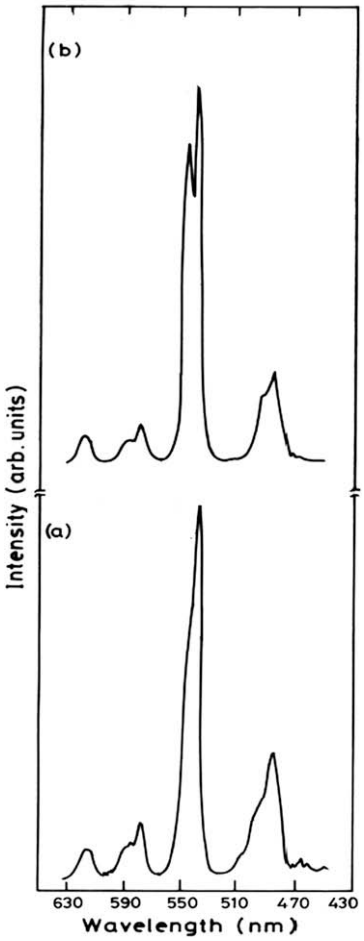

Fig. 10. Emission spectra of $LaSr_5Y_{0.9}Tb_{0.1}Mg(BO_3)_6$ recorded for two different excitation wavelengths: (a) λ_{exc} = 254 nm and (b) λ_{exc} = 238 nm.

directly. As a result, no sensitizer(s) like Ce^{3+} is required which is highly unstable when heated in air at high temperatures.

(b) The Tb^{3+} ions in the finally formed hexaborates are highly stable when heated in air at room and at high temperatures (as revealed by thermal studies (TG/DT) on the formed product). Hence, these borate phosphors do not cause any stability problem during the baking process of lamp fabrication.

(c) The optimum concentration of Tb^{3+} ion in these borates ($x = 0.5$) required to cause efficient green emission in these borates is very reasonable when compared to the Tb^{3+} concentration of the standard commercial phosphors $LaCePO_4:Tb^{3+}$ and $CeMgAl_{11}O_{19}:Tb^{3+}$ which are currently in use. The optimum concentration of Tb required in the case of aluminate phosphors is close to 33 mol% and in phosphate it is close to 15 mol% which is high. This is known by calculating the overall weight of Tb per kg of all these phosphors. Hence, the Tb^{3+}-ion content in the hexaborate lattices is low when compared to the standard green phosphors. In addition, many hexaborate hosts for Tb^{3+}-activation contain only less expensive non-rare earth materials and hence cost-reduction is highly possible.

(d) All these hexaborate phosphors can be synthesized at lower temperatures ($\leqslant$1000 °C) under mild-reducing atmospheres, when compared to the standard aluminate and phosphate green phosphors. Hence, all these factors lead to cost-reduction of the phosphors and hence the lamps based on these phosphors. All these borates are stable to dispersion in aqueous solutions.

(e) The narrow particle size distribution (5–15 μm), moderate density values ($\sim$3.7 g ml^{-1}) and the flexible crystal structure of the borate lattice are the other advantages of these borate phosphors.

(f) Our recent work on this system of borates shows that, after blending with $Zn_2SiO_4:Mn^{2+}$ phosphor, the resultant blend gives better results in terms of color purity and color temperature under excitation with 172 nm (Xe discharge in PDPs) and hence suitable for application in plasma display panels [21].

4. Conclusions

Several new green phosphors have been identified in Tb^{3+}-activated hexaborates of the type $Sr_6M_{1-x}Tb_xM'(BO_3)_6$ [M = M′ = Gd, Y], $Sr_6TbM'(BO_3)_6$ [M′ = Al, Ga, In, Sc] and $LaSr_5Y_{1-x}Tb_xMg(BO_3)_6$ where $0.05 \leqslant x \leqslant 1.0$. These compounds are synthesized by the solid state reaction under reducing atmosphere and are characterized by XRD, TG/DT, density, particle size analysis and photoluminescence techniques. The single phase crystalline compounds synthesized at temperatures $\leqslant$1000 °C, give good density, and narrow particle size. Photoluminescence excitation and emission studies on these borates show that the excitation and emission features are similar to the existing aluminate, borate and phosphate green phosphors applied in tri-color lpmv lamps. The hexaborate system has several advantages over the standard green phosphors *viz*., direct excitation with 254 nm, no sensitizer like Ce^{3+} ion which is unstable, low temperature for synthesis, stability of Tb^{3+}-ion at low and high temperatures in air and hence these borates are identified as efficient new alternatives to the existing commercial green phosphors for use in tri-color lpmv lamps.

Acknowledgements

I am grateful to Prof. G.V. Subba Rao for leaving this paper generously to me to communicate as single author. Thanks are due to Mr. K. Athinarayanasamy and Dr. A. Mani for XRD studies, Dr. V. Sundaram for TG/DT measurements, Mr. L.K. Srinivasan for particle size analysis, Dr. Sainkar, NCL, Pune for SEM studies, Mr. A. Muthukumaran for FT-ir studies, Mr. N. Ramakrishnan for typing the manuscript and Mr. SP. Pandurangan for drawings.

References

[1] B.M.J. Smets, Mater. Chem. Phys. 16 (1987) 283.
[2] G. Blasse, E.C. Grabmaier, Luminescent Materials, Springer-Verlag, Berlin, 1994.
[3] T. Justel, H. Nikol, C. Ronda, Angew. Chem., Int. Ed. 37 (1998) 3084.
[4] K.I. Schaffers, T. Alekel III, P.D. Thompson, J.R. Cox, D.A. Keszler, J. Am. Chem. Soc. 112 (1990) 7068.
[5] K.I. Schaffers, T. Alekel III, P.D. Thompson, J.R. Cox, D.A. Keszler, Chem. Mater. 6 (1994) 2014.
[6] P.D. Thompson, D.A. Keszler, Chem. Mater. 6 (1994) 2005.
[7] R. Sankar, G.V. Subba Rao, J. Alloys Compd. 281 (1998) 126.
[8] G.V. Subba Rao, R. Sankar, US Pat. 6090310 (2000).
[9] G. Blasse, A. Bril, Philips Res. Rep. 22 (1967) 481.
[10] R.C. Ropp, J. Electrochem. Soc. 115 (1968) 531.
[11] J. Fu, M. Kobayashi, J.M. Parker, J. Lumin. 128 (2008) 99.
[12] J.M.P.J. Verstegen, J.L. Sommerdijk, J.G. Verriet, J. Lumin. 6 (1973) 425.
[13] X. Bai, G. Zhang, P. Fu, J. Solid State Chem. 180 (2007) 1792.
[14] B. Saubat, C. Fouassier, P. Hagenmuller, Mater. Res. Bull. 16 (1981) 193.
[15] B. Grobelna, J. Alloys Compd. 440 (2007) 265.
[16] M.J.J. Lammers, G. Blasse, Mater. Res. Bull. 19 (1984) 759.
[17] J.L. Ryan, C.K. Jorgensen, J. Phys. Chem. 70 (1966) 2845.
[18] F. Varsanyi, G.H. Dieke, Phys. Rev. Lett. 1 (1961) 442.
[19] T. Hayakawa, N. Kamata, K. Yamada, J. Lumin. 68 (1996) 179.
[20] X. Zhang, J. Zhang, L. Liang, Q. Su, Mater. Res. Bull. 40 (2005) 281.
[21] R. Sankar, India Patent (Applied), 2007.